



24th ABCM International Congress of Mechanical Engineering  
December 3-8, 2017, Curitiba, PR, Brazil

24th COBEM - 2017

## COBEM-2017-2661

# INFLUENCE OF TOOL PATH OPTIMIZATION IN ADDITIVE MANUFACTURING BASED ON MATERIAL EXTRUSION

**N. Volpato**

**T. Zanotto**

**T. Weller**

Universidade Tecnológica do Paraná (UTFPR), R. Dep. Heitor Alencar Furtado, 5000 – Curitiba-Pr, CEP 81280-340,  
thiagozanotto@hotmail.com, nvolpato@utfpr.edu.br, weller@utfpr.edu.br

**Abstract.** Material Extrusion is one of the additive manufacturing (AM) principle where a filament of material, produced by an extrusion nozzle, is deposited following a tool path to fill in the areas of each layer. In this principle, it is observed that the extrusion nozzle must stop extrusion and jump from one point to another to start a new deposition (head repositioning). This study aims to evaluate the influence of path planning optimization, mainly head repositioning, on mechanical properties, dimensional and building time of specimens manufactured using a 3D Cloner printer. An experiment involving an interruption of extrusion nozzle was also performed. This was designed to analyze the influence of the idle time during the material deposition on the material properties. The results in the tensile and 3-point bending test showed small variation between the different path planning. On the other hand, for the experiment with interruption of the extrusion nozzle, the variation reached up to 46% (decrease in flexural strength). Regarding the building time between the different path planning tested, it was noticed a difference up to 42.7%. In the dimensional evaluation, it was observed only a small variation between the tested methods.

**Keywords:** path optimization, process planning, additive manufacturing

## 1. INTRODUCTION

The additive manufacturing (AM), also referred to as 3D printing, is a manufacturing process which, using data directly obtained from a 3D geometric model, adds material layer upon layer, unlike the material removal manufacturing (ISO/ASTM 52900:2015). The AM based on Material Extrusion principle uses an extrusion head that moves in XY plan by depositing a material filament that will fill in the area in each layer. At the end of each layer, the platform moves downward a distance equal of the layer thickness, and a new layer of material is added. The Fused Deposition Modeling (FDM) was the first material extrusion AM technology, which was developed by Stratasys Ltd. Time is important for this kind of AM technology, because the extrusion nozzle needs to produce a filament of material that has to fill in the entire areas of each layer (Volpato *et al.*, 2015). According to Volpato and Carvalho (2017), the main tasks of the AM process are: 3D geometric model, path planning, manufacturing process and post processing. In this work, the main interest is the path planning, which is the process of defining the filling path for the 2D area(s) of each layer. Usually, the filling is not performed in a continuous path and the extrusion nozzle needs often to be repositioned to restart the process. This work aims to study the influence of path planning optimization, considering mainly head repositioning, on mechanical properties, dimensional and build time for specimens manufactured using a 3D Cloner printer, which is based on the material extrusion principle.

## 2. HEAD REPOSITIONING

In the FDM technology, the material deposition is usually performed by following first the contours (C) of the part and then by filling in the internal areas of each contour. The filling is usually performed using zigzag strategy (raster filling), containing a start and an endpoint (Volpato *et al.*, 2015). Figure 1 shows schematically a path planning of a layer with a possible sequence of contours and raster fillings. In contour with a non-convex polygon, a single Continuous Raster Segment (CRS) is not sufficient to fill in the entire area (Agarwala *et al.*, 1996). More than one CRS is required in this case. For instance, the C3 in Fig. 1 requires three CRSs to be completely filled. To go from one end point of a deposition path to the next start point, the machine performs rapid movements without material deposition, defined here as head repositioning (also known as nonproductive airtime or jump). These repositioning, which are drew as dashed lines in Fig.

1, represent discontinuity in the filling deposition path. Then, a head repositioning is necessary when jumping from one C to another, from one C to a CRS or from one CRS to another (Volpato *et al.*, 2015).

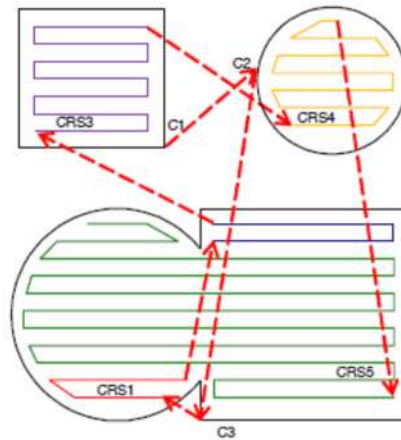


Figure 1. Path planning deposition and repositioning for the material extrusion principle (Volpato *et al.*, 2015)

### 3. MATERIALS AND METHODS

The 3D Cloner printer was used to fabricate tensile and flexural test specimens with polylactic acid (PLA), which has the filament diameter of 1.75mm. The tensile and flexural specimen's dimensions (Fig. 2) follow the ASTM D638-14 (American Society for Testing and Materials) and ASTM D790-10, respectively. Five specimens were fabricated for each proposal path planning (described below). The tensile and the 3-point bending tests were carried out in EMIC TM (DL 1000) test machine.

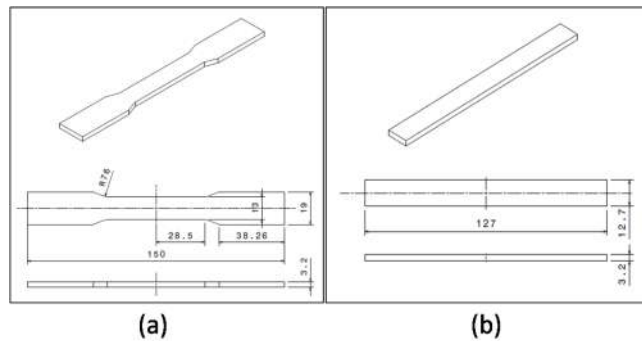


Figure 2. Dimensions (mm) of the (a) tensile and (b) flexural specimens

The process parameters used can be seen in the Tab. 1 and they were kept constant for all proposed methods.

Table 1. Process parameter used for all proposed methods.

Parameters	Values
Nozzle diameter	0,4mm
Filament diameter	1,75mm
Fill density	100%
Layer thickness	0,25mm
Head speed	40mm/min
Printing temperature	200°C
Raster angle	0°/90°

The fill density parameter was set to 100% in order to deposit filaments as close as possible to each other - thus allowing the study of the lateral adhesion between them. This was done because the software does not provide a specific

parameter to control the gap between the filaments. Setting it to 100% means that the material density inside the object is maximum. In contrast, a 0% value indicates a hollow piece (Bratl, 2013).

The building time was registered by the estimated time from the 3D Cloner printer. The dimensional measurements were performed using a Mitutoyo digital caliper of 150mm, with resolution of 0.01mm.

### 3.1 Proposed path planning strategies to study optimization

In this work, three different path planning strategies were defined. The first one was called non-optimized intercalated, the second optimized sequential and the last one optimized intercalated strategy. The first and third path planning strategies were chosen based on the common use of these strategies in 3D low-cost printer. The second one was chosen because it is commonly used in Stratasys machine.

The optimization heuristic used in both strategies was the greedy method. This heuristic starts from the origin point, then, in every step, it adds to the route the point belonging to a C that has not been visited yet and whose distance to the last point visited is the smallest possible. After it has visited all Cs, the procedure is repeated searching for the raster segments. When the nearest point of a CRS is found, the end point of this CRS is automatically included as being the next point. The procedure then carries on searching for the next CRS that has not been visited yet (Volpato *et al.*, 2013).

The tensile and flexural specimens were fabricated with other two pieces, called shims (dimensions: 15x30x3.2 mm), on the same printing platform (Fig. 3). These shims had the objective to increase the number of Cs and CRSs in each layer, thus increasing the possibility of the path planning optimization influencing the results.

The blue contours (lines) around the specimen and the shims observed in Fig. 3 are called skirts. The skirt is used to purge the extrusion nozzle, thus avoiding errors in the beginning of filament deposition in the specimens. It is worth mentioning that these contours were made only in the first layer and just before the first C of each part.

#### 3.1.1 Non-optimized intercalated path planning strategy (CRCR-NO)

In this strategy, the sequence of deposition is done by first adding the external C of the part and then the CRSs belonging to this specific C. The notation CRCR means a contour-C followed by a raster segment-R, then another C, followed by another R, and so on, and NO means not applying optimization. If there is any internal C (or Cs) in the part, it need to be deposited first and only after that, all respective CRSs can be deposited. This sequence is repeated until the deposition of all Cs and CRSs of the layer. There is no optimization of the head repositioning for this method, so the C and CRS sequence for all layers are repeated. Figure 3 shows the path planning of the first and the beginning of the second layer for this method. The raster angle adopted was zero degrees related to the X axis.

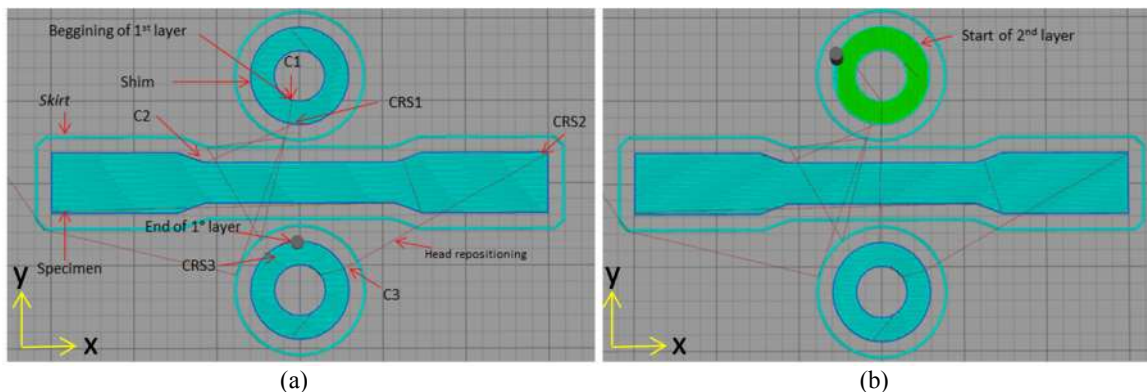


Figure 3. Path planning deposition for CRCR-NO: (a) first layer and (b) second layer

#### 3.1.2 Optimized sequential path planning strategy (CCRR-O)

The path planning of this method involves depositing all Cs of a layer first and only then carry on with the CRSs. Figure 4 shows the path planning of the first layer using this proposed method. The greedy method was used to optimize the head repositioning (CCRR-O, where O means applying optimization).

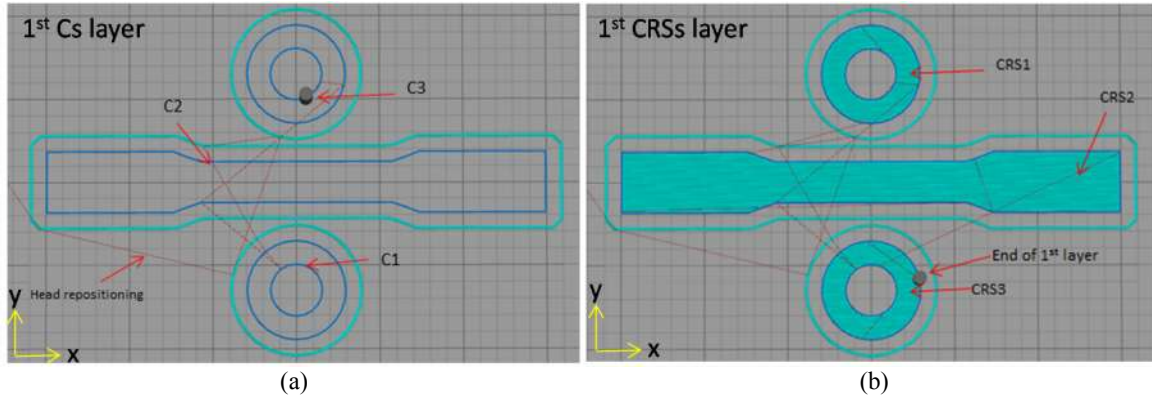


Figure 4. Path planning deposition for CCRR-O: (a) all Cs firsts and then (b) all CRSs of the first layer

### 3.1.3 Optimized intercalated path planning strategy (CRCR-O)

This strategy follows the same path planning of the CRCR-NO, i.e., to deposit an external C and then the CRS of this external C (considering that there is no internal C inside the first one). The difference is that optimization of head repositioning was used based on the greedy method.

### 3.2 Path planning considering an intentional extrusion break

An additional experiment was carried out introducing an interruption of the extrusion during filament deposition of the CRS corresponding to the transverse layers ( $90^\circ$  raster angle) of both tensile and flexure specimens. In Fig. 5, an illustration of this method is presented. The main goal of this experiment was to evaluate the influence of time on the adhesion between filaments of neighboring CRSs, since optimization can lead to variation of the filling time of these CRSs.

The shims were not manufactured together in these experiments and the non-optimized intercalated path planning strategy (CRCR-NO) was used.

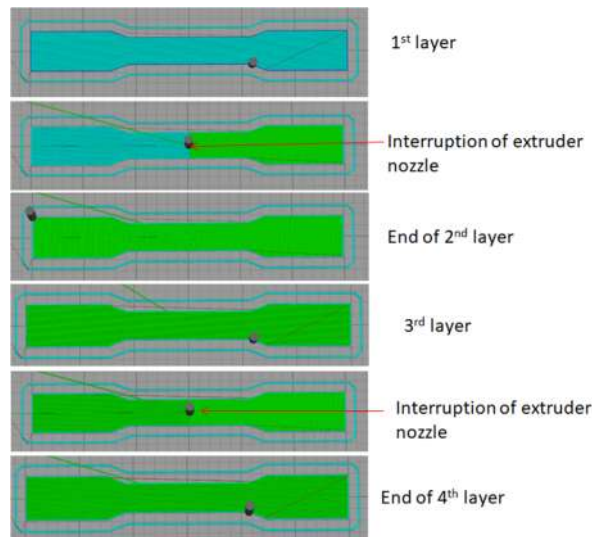


Figure 5. Illustration of path planning deposition with the intentional interruption of extrusion nozzle

As can be seen in Fig. 5, the deposition in the odd layers (raster angle  $0^\circ$ ) is done normally, but in the even layers there is an interruption of the material extrusion in the center of the part (X and Y axis). After the interruption, the extrusion nozzle is displaced to the platform corner and starts moving along the Y axis for 65 seconds. The purpose of this was to avoid irradiation of the nozzle in the specimen during this idle time. The 65 seconds (P65) was chosen because it corresponds to the estimated time to deposit 50% of the CRS in the transverse layer. Additionally, specimens were

fabricated under these same conditions but with an interruption of 17 seconds (P17). This was an estimated time for a return of the extrusion nozzle to its original position, which, in this case, is located in the upper left corner of the platform.

After the tensile and 3-point bending tests, the fracture morphology of the CRCR-NOP17 and CRCR-NOP65 specimens were analyzed using a TM 3000 (Hitachi) scanning electron microscopy (SEM).

#### 4. RESULTS AND DISCUSSION

Table 2 presents the building time to manufacture one specimen (tensile and flexure) for the proposed methods. The variations (%) presented in this table, correspond to the comparison of the CCRR-O and CRCR-O methods with the CRCR-NO one.

Table 2. Comparison of building time for the proposed methods.

Specimens	CRCR-NO (s)	CCRR-O (s)	Variation (%)	CRCR-O (s)	Variation (%)
Tensile	3139	4452	+41,8	3135	-0,13
Flexure	2392	3377	+41,2	2383	-0,38

Based on these results, it can be observed that the time variation between the CRCR-NO and CRCR-O methods was not significant. On the other hand, the building time increased about 41% in the manufacture of the tensile and flexural specimens for the CCRR-O, when compared to the CRCR-NO method. This fact is related to the path planning applied by this method (CCRR-O), which normally generates more idle movements, since it must go through all Cs before starting the CRSs.

In Tab. 3, the dimensional results were presented for all methods tested including the one with interruption of the extrusion.

Table 3. Dimensional results for all proposed methods.

Method	Tensile Specimen		Flexure Specimen		
	Width (mm)	Thickness (mm)	Width (mm)	Thickness (mm)	Length (mm)
CRCR-NO	13.26±0.09	3.21±0.05	12.87±0.07	3.19±0.04	126.87±0.10
CCRR-O	13.26±0.09	3.25±0.04	12.74±0.07	3.20±0.05	126.47±0.39
CRCR-O	13.44±0.44	3.19±0.02	13.12±0.24	3.17±0.08	127.15±0.05
CRCR-NOP17	13.21±0.04	3.31±0.02	12.68±0.03	3.29±0.02	126.69±0.04
CRCR-NOP65	13.15±0.06	3.36±0.04	12.71±0.07	3.28±0.06	126.73±0.16

Based on the results for the tensile specimens, it can be verified that the maximum variation in the width was approximately 3.4% in the CRCR-O method, in relation to the nominal dimensions. In the thickness, the highest variation was approximately 5% for the P65 method. Considering the average and dispersion of the values, the dimensional differences between the CRCR-NO, CCRR-O and CRCR-O methods were not significant.

For the flexural specimens, the CRCR-O method had the largest width variation (3.3%), when comparing with the nominal values. The CRCR-NOP17 and CRCR-NOP65 methods had the highest thickness variation (2.8% and 2.5%, respectively). In the length, the variation found was not significant, not exceeding 0.5% in relation to the nominal dimension.

The tensile test results are presented in Fig. 6. The highest value (average) of tensile stress at break was 50.4 MPa when the specimens were manufactured by the CCRR-O method. For the CRCR-O method, there was a decrease of 7% when compared to the CCRR-O method. Considering the mean and standard deviation of the results for the CRCR-NO, CCRR-O and CRCR-O methods, the values are comparable and had little variation among them.

Comparing the tensile strength of the CRCR-NOP17 and the CRCR-NO methods, there was a decrease of approximately 25%, whereas for the CRCR-NOP65, the decrease was approximately 35%. As the only process change in the two cases was the interruption time during the deposition, it can be considered that the adhesion between the neighboring filaments was not efficient and this was the reason for this decrease in the material property. This corroborates with the results found by Gurralla and Regalla (2014), in which they concluded that the manufacturing strategy and the environment temperature are key factors that affect both the quality and the bond strength between filaments. Once deposited, each filament should solidify as quickly as possible in order to avoid deformation due to the gravity and mass of the material deposited on top. However, the filament must remain heated enough to ensure adequate bonding between its neighbor.

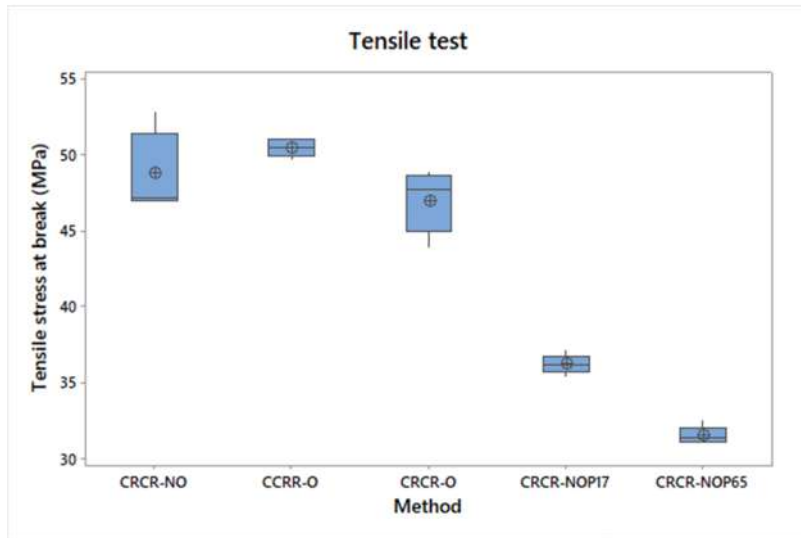


Figure 6. Tensile test results

The results presented above show that there was little variation between the methods with and without optimization of the head repositioning, considering the manufacturing conditions of this study. However, for the methods with interruption, a considerable variation in the tensile strength was observed. These results indicate the region where the interruption occurred became weaker. Bearing that in mind, it is possible to admit that, if a path optimization increases the deposition time between neighboring filaments, the part produced may have a negative impact in the mechanical properties. However, analyzing head reposition optimizations, one could expect that the time between neighboring CRSs would be shorter, and, therefore, this would not negatively imply the mechanical properties of the parts.

Figure 7 shows the results for the 3-point bending tests for the proposed methods. It can be observed that the highest average of flexure stress at break was 84.64 MPa using the CCRR-O method. There was a decrease of approximately 7% and 10% for the CRCR-NO and CRCR-O methods, respectively, when compared to the CCRR-O method. However, considering the mean and standard deviation the results obtained were close.

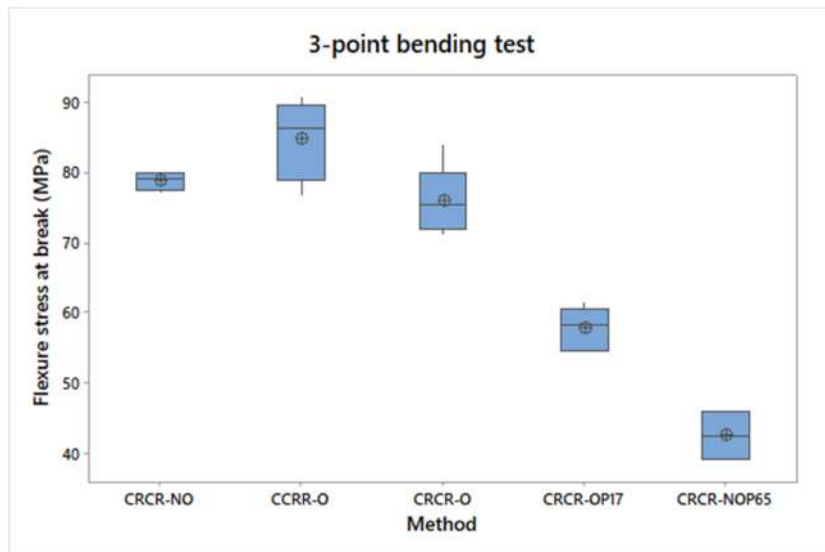


Figure 7. 3-point bending test results

There was a decrease in flexure strength of approximately 26% for the CRCR-NOP65 method when compared to CRCR-NOP17. This shows that increasing the interruption time from 17 to 65 seconds has a direct correlation with the decreasing in strength. Comparing P17 and P65 with CRCR-NO, the decrease in flexure strength was approximately 26% and 46%, respectively. As in the tensile tests, it is evident that the interruption time during filament deposition had a

significant influence on the mechanical behavior of the material. This time adversely affected the adhesion between the adjacent filaments.

Figure 8 shows some specimens after the tensile and the 3-point bending tests for the methods CRCR-NOP17 e CRCR-NOP65. It can be seen that, for both methods, all fractures in the specimens occurred exactly in the region of the interruption (center of the specimen). There is an evident difference in the fracture between the P17 and P65 methods. For the P65 specimen, some longitudinal filaments become exposed after rupture. These filaments are from the layers above and below the interrupted layer. This behavior suggests that, due to the long interruption time in the transverse layers, the previous layers could be cooler, thus causing also an inefficient adhesion of the filaments between layers.

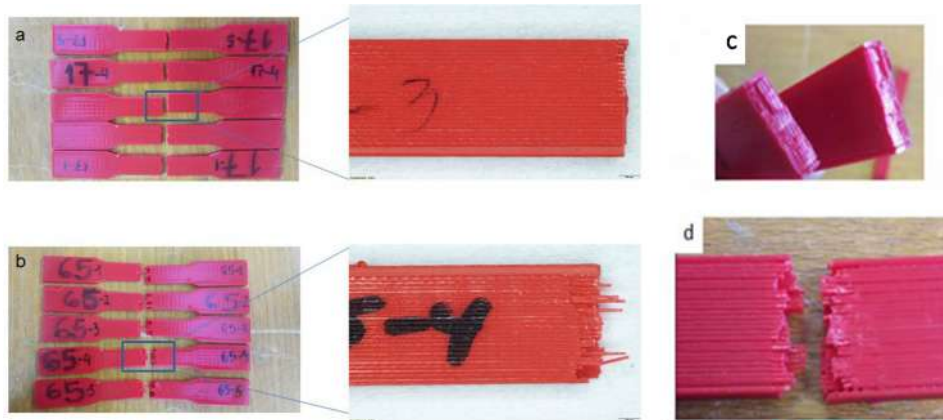


Figure 8. Specimens after tensile and flexural tests: (a) CRCR-NOP17 tensile specimens, (b) CRCR-NOP65 tensile specimens, (c) CRCR-NOP17 flexure specimen and (d) CRCR-NOP65 flexure specimen

The SEM images of the fractured specimens obtained by the CRCR-NOP17 and CRCR-NOP65 methods are shown in Fig. 9. The fractures morphologies showed that the layers which are close to the machine platform have a better adhesion between the filaments when compared to those of the top layers. In the P65 specimen, some filaments of quite circular cross section can be found, which is different from the expected, which would be closer to an ellipse. This indicates a filament that did not have a good interaction with its neighbors (both laterally and vertically). This implies that sliding might occur between the filaments of adjacent layer in this region, i.e., bad adhesion between layers.

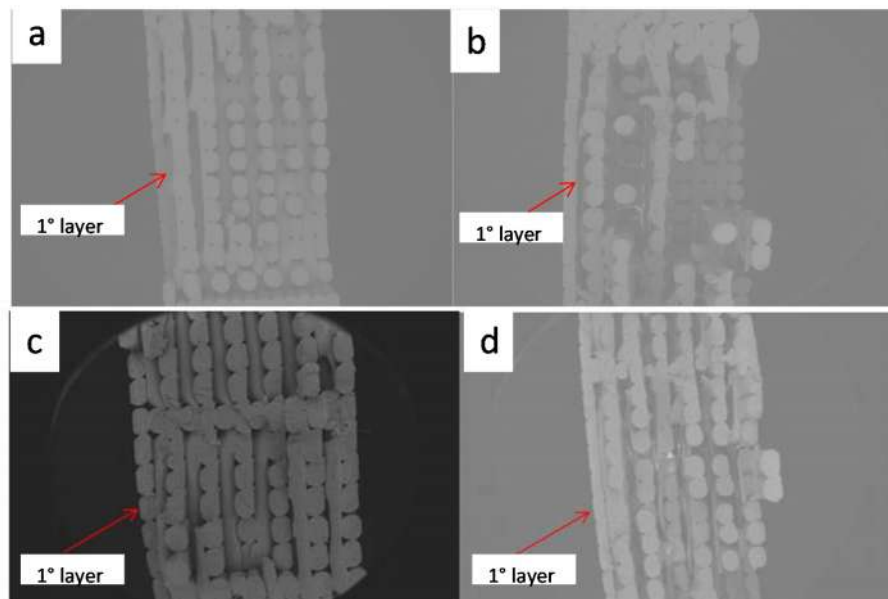


Figure 9. SEM images of the fractured surfaces: (a) CRCR-NOP17 and (b) CRCR-NOP65 tensile specimens, and (c) CRCR-NOP17 and (d) CRCR-NOP65 flexure specimens

The SEM results corroborates with the studies of Sun *et al.* (2003), that showed improvement in the filaments adhesion when compared the first and last deposited layers. Sun *et al.* (2008) also report that the lower layers of the parts are kept at higher temperature for a longer period of time when compared to the upper layers. The growth of the "neck" between the filaments is expected to be higher in the lower layers than in the upper layers. This can be observed in Fig. 9a, when comparing the first and the last layer.

## 5. CONCLUSION

This work explored the influence of different paths planning (optimization of head repositioning) on the mechanical properties of specimens produced with the material extrusion AM process.

In the dimensional results, little variation was observed when comparing the path planning with and without optimizations.

The tensile and flexural results showed that the CCRR-O method obtained slight better mechanical properties compared to the others paths planning tested. However, considering the mean and standard deviation, there is also little difference between the methods.

For the experiment with the intentional interruption of the extrusion (17 and 65 seconds) in the center of the part, a great decrease in the mechanical properties (46% in the flexural strength) was found when compared to those without interruption. In the SEM analysis, it was possible to observe that the layers did not suffer adequate adhesion, considering the results of tensile and flexural tests. This behavior is caused by the different temperatures in which the layers were exposed.

Considering the geometry and the method of optimization (greedy) tested, the influence on the mechanical properties was small. However, a point to be considered is that, the strategy (optimized or not) which results in taking longer time to deposit neighboring raster segments will negatively affect the mechanical properties of the part.

## 6. REFERENCES

- Agarwala, M.K., Jamalabad, V.R., Langrana, N.A., Safari., A, Whalen, P.J. and Danforth, S.C., 1996. Structural quality of parts processed by fused deposition. *Rapid Prototyping Journal*, Vol. 2, p. 4-19.
- ATSM D638-14, 2014. Standard test methods for tensile properties of plastics, American Society for testing and Materials (ASTM) International.
- ATSM D790-10, 2010. Standard test methods for flexural properties unreinforced and reinforced plastics and electrical insulating materials, American Society for testing and Materials (ASTM) International.
- Bratl, M., 2013. *Customizable Personal Manufacturing*. Master Thesis, Fachhochschule Der Wirtschaft , Hannover.
- ISO/ASTM 52900, 2015. *Additive manufacturing - General principles – Terminology*.
- Gurrula, P. K. and Regalla, S. P., 2014. Part strength evolution with bonding between filaments in fused deposition modelling: This paper studies how coalescence of filaments contributes to the strength of final FDM part. *Virtual and Physical Prototyping*, Vol. 9, p. 141-149.
- Sun, Q., Rizvi, G., Bellehumeur, C. and Gu, P., 2003. Experimental Study of the Cooling Characteristics of Polymer Filaments in FDM and Impact on the Mesostructures and Properties of Prototypes. In *Solid Freeform Fabrication Symposium*, Austin.
- Sun, Q., Rizvi, G.M., Gu, P. and Bellehumeur, C.T., 2008. Effect of processing conditions on the bounding quality of FMD polymer filaments. *Rapid Prototyping Journal*, Vol. 14, p. 72-80.
- Volpato, N., Nakashima, R.T., Galvão, L.C., Barboza, A.O., Benevides, P.F. and Nunes, L.F., 2013. Reducing repositioning distances in fused deposition-based processes using optimization algorithms. In *High Value Manufacturing: Advanced Research in Virtual and Rapid Prototyping: Proceedings of the 6th International Conference on Advanced Research in Virtual and Rapid Prototyping*. Leiria, Portugal.
- Volpato, N., Galvão, L.C., Nunes, L.F. and Scanavini, L.G., 2015. Combining Heuristics for Tool-path Optimization in Additive Manufacturing. In *Computer-Aided Production Engineering - CAPE Conference, Edinburgh. Proceedings of the 23rd CAPE Conference*. Edinburgh, University of Edinburgh.
- Volpato, N. and Carvalho, J. de., 2017. Introdução à manufatura aditiva ou impressão 3D. In *Manufatura Aditiva – Tecnologias e aplicações da impressão 3D*. São Paulo, Blucher.

## 7. RESPONSIBILITY NOTICE

The authors are the only responsible for the printed material included in this paper.